Taylor & Francis
Taylor & Francis Group

Check for updates

RESEARCH PAPER

Rbm24 regulates inner-ear-specific alternative splicing and is essential for maintaining auditory and motor coordination

Longqing Zheng[a], Huijun Yuan[b], Mengkai Zhang[a], Cuicui Wang[b], Xuemin Cai[a], Jing Liu[a,c], and Xiu Qin Xu [a]

[a]The Institute of Stem Cell and Regenerative Medicine, School of Medicine, Xiamen University, Xiamen, China; [b]Medical Genetics Center, Southwest Hospital, Army Medical University, Chongqing, China; [c]Shenzhen Research Institute, Xiamen University, P.R. China

ABSTRACT

Tissue-specific alternative splicing (AS) is emerging as one of the most exciting types of mechanisms associated with organ development and disease. In the auditory system, many hearing-related genes undergo AS, and errors in this process result in syndromic or non-syndromic hearing loss. However, little is known about the factors and mechanisms directing AS in the inner ear. In the present study, we identified a novel RNA-binding protein, Rbm24, which was critically involved in regulating inner-ear-specific AS. Rbm24 deletion resulted in hearing loss and defects in motor coordination. Global splicing analysis showed Rbm24 was required for correct splicing of a subset of pre-mRNA transcripts with essential roles in stereocilia integrity and survival of hair cells. Furthermore, we identified that Rbm24 directly regulated the splicing of Cdh23, a known disease gene responsible for human Usher syndrome 1D and non-syndromic autosomal recessive deafness DFNB12. In conclusion, our findings demonstrated that Rbm24 was a critical factor in regulating inner-ear-specific splicing and maintaining the hearing and motor coordination function of the inner ear. Our data not only offer mechanistic insights but also provide functional annotation of Rbm24 splicing targets that contribute to hearing loss.
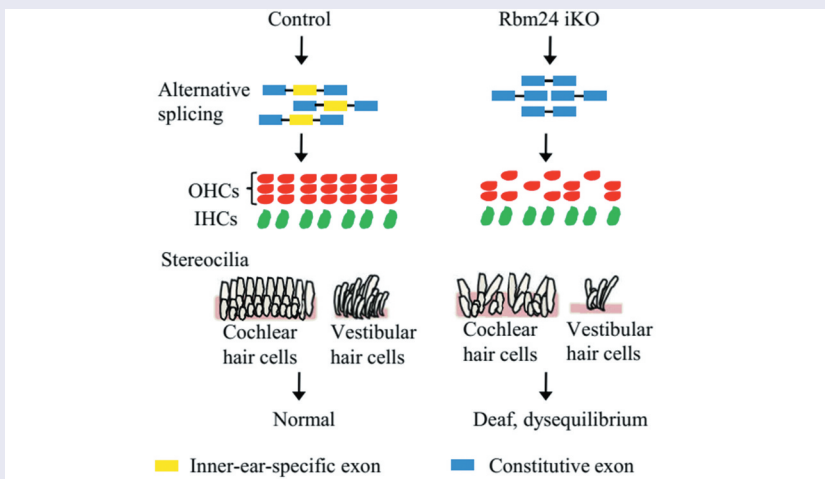
Our study identified that Rbm24 is a critical factor in regulating inner-ear-specific splicing. Rbm24 deletion disrupts global alternative splicing and results in outer hair cell (OHCs) degeneration and hair bundle loss, which led to hearing loss and dysequilibrium.

CONTACT Xiu Qin Xu ✉ xuxq@xmu.edu.cn ▣ The Institute of Stem Cell and Regenerative Medicine, School of Medicine, Xiamen University, Xiamen 361100, China

Supplemental data for this article can be accessed here.

Introduction

Sensorineural hearing loss is one of the most frequent congenital diseases affecting ~1 in 1,000 newborns worldwide [1]. More than 50% of cases of congenital hearing loss can be attributed to genetic factors [2]. As research progresses, more and more hearing-related genes are being identified [3]. Notably, studies on hearing-related genes have shown that alternative splicing (AS) plays important roles in the development and function of the inner ear, and errors in this process result in syndromic or non-syndromic hearing loss [4]. However, the AS factors and mechanisms directing inner-ear-specific splicing are still relatively sparsely studied [4]. Moreover, the specific biological processes controlled by the inner-ear-specific exons are also not well understood.

The inner ear is a structurally complex vertebrate organ built to encode sound, motion, and orientation in space [5]. It can be roughly divided into the vestibular and cochlear components; where the vestibular system detects head movements and the cochlea is responsible for sound perception [5]. In the inner ear, the process of auditory and motion transduction is dependent on the proper function of sensory hair cells [6]. Each hair cell projects an array of actin-filled stereocilia from its apical cell surface, which are organized into rows and served an important role in auditory transduction [7]. Hair cell degeneration and stereocilia defects are associated with numerous hearing and motor coordination defects in humans [8,9].

We have previously reported that RNA-binding motif protein 24 (Rbm24) is enriched in human embryonic cells-derived cardiomyocytes and is highly expressed in the human and mouse heart [10]. Studies from our group and others have further characterized the functional roles of Rbm24 in the development of the heart and in heart disease [11–14]. Interestingly, Rbm24 is not only highly expressed in the striated muscle, it is also expressed in the developing otic vesicle and in postnatal mice inner ear hair cells [15,16]. However, whether Rbm24 functions as a splicing regulator which serves a functional role in the inner ear is unknown.

A previous study suggested that Rbm24 null mice were embryonic lethal [12]. To explore the potential role of Rbm24 in the inner-ear, we generated a tamoxifen (TMXF) inducible knockout (iKO) mouse. Rbm24 deletion resulted in hearing loss and motor coordination defects, and the hair cells and stereocilia were degenerated. Global splicing analysis in Rbm24 knockout mice revealed impaired splicing of pre-mRNAs with essential roles in stereocilia integrity and survival of hair cells. Furthermore, we showed that Rbm24 directly regulated the inclusion of the Cdh23 inner-ear-specific exon. These results indicated that Rbm24 was a critical factor responsible for regulation of inner-ear-specific splicing and maintenance of inner ear function.

Materials and methods

Ethics and animal care

All animal experiments were approved by the Institutional Animal Care and Use Committee (IACUC) of Xiamen University (Xiamen, Fujian, China; approval ID: SCXK2013-0006). Mice were sacrificed by placing them in a box containing 100% CO_2 for 5 min or by cervical dislocation.

Generation of Rbm24 iKO mice

Generation of Rbm24$^{loxp/loxp}$ mice performed as described in our previous study [14]. Rbm24$^{loxp/loxp}$ mice were then crossed with a transgenic line UBC-CreER^{T2} (Shanghai Model Organisms Centre), in which the recombinase activity is activated by 4-hydroxytamoxifen, to generate the Rbm24 iKO mice. The mouse breeding scheme is shown in Fig. 1D. Genotyping of mouse genomic DNA was performed using PCR, with different Rbm24 alleles and Cre PCR primers as described in our previous study [14]. Control (Rbm24$^{loxp/loxp}$) and iKO (UBC-CreER^{T2}, Rbm24$^{loxp/loxp}$) mice were administered TMXF at 2 months of age at a dosage of 100 mg per kilogram of body weight for 5 days. TMXF (MCE, New Jersey, USA) was dissolved in corn oil (Aladdin, ShangHai, China) at 20 mg/ml.

Tissue preparation

Mice were sacrificed and decapitated to expose the dorsal surface of the base of the skull. Inner ears were dissected and fixed in cold 4% paraformaldehyde overnight and then decalcified in 150 mM EDTA solution for 5 days at 4°C. Inner ears were then embedded in OCT (Leika, USA) and processed for frozen sectioning or dissected for wholemount immunostaining.

Immunofluorescence staining

Cryosections of the inner ear were permeabilized using 0.25% TritonX-100 in PBS and then blocked in 3% BSA (Boster Biological Technology, Pleasanton, CA, USA) for 1 h at room temperature. Subsequently, sections were incubated with primary antibody overnight at 4°C, then washed 3 times with PBS and incubated with AlexaFluor® 488 conjugated secondary antibody (1:500; Invitrogen; Thermo Fisher Scientific, Inc. California, USA) at room temperature for 1 h. After washing with PBS, the sections were counterstained with DAPI (1:5,000, Sigma-Aldrich; Merck KGaA-Aldrich; Merck KGaA, Darmstadt, Germany) and mounted on cover slips by adding one drop of anti-fade solution (Boster Biological Technology, Pleasanton, CA, USA) to the area of tissues. Wholemount immunostaining of vestibular or cochlear sensory organs was performed using a similar protocol with some minor modifications. Primary antibodies used were anti-myo7a (1:200; Clinisciences, Montrouge, France) and anti-Rbm24 (1:500; Abcam, UK). Actin in stereociliary bundles was labelled with Alexa 488-conjugated phalloidin (1:50; Invitrogen; Thermo Fisher Scientific, Inc. California, USA). Images were captured by confocal laser scanning fluorescence microscopy (Olympus FV1000; Olympus Corporation, Japan) or fluorescence microscopy (Olympus IX81).
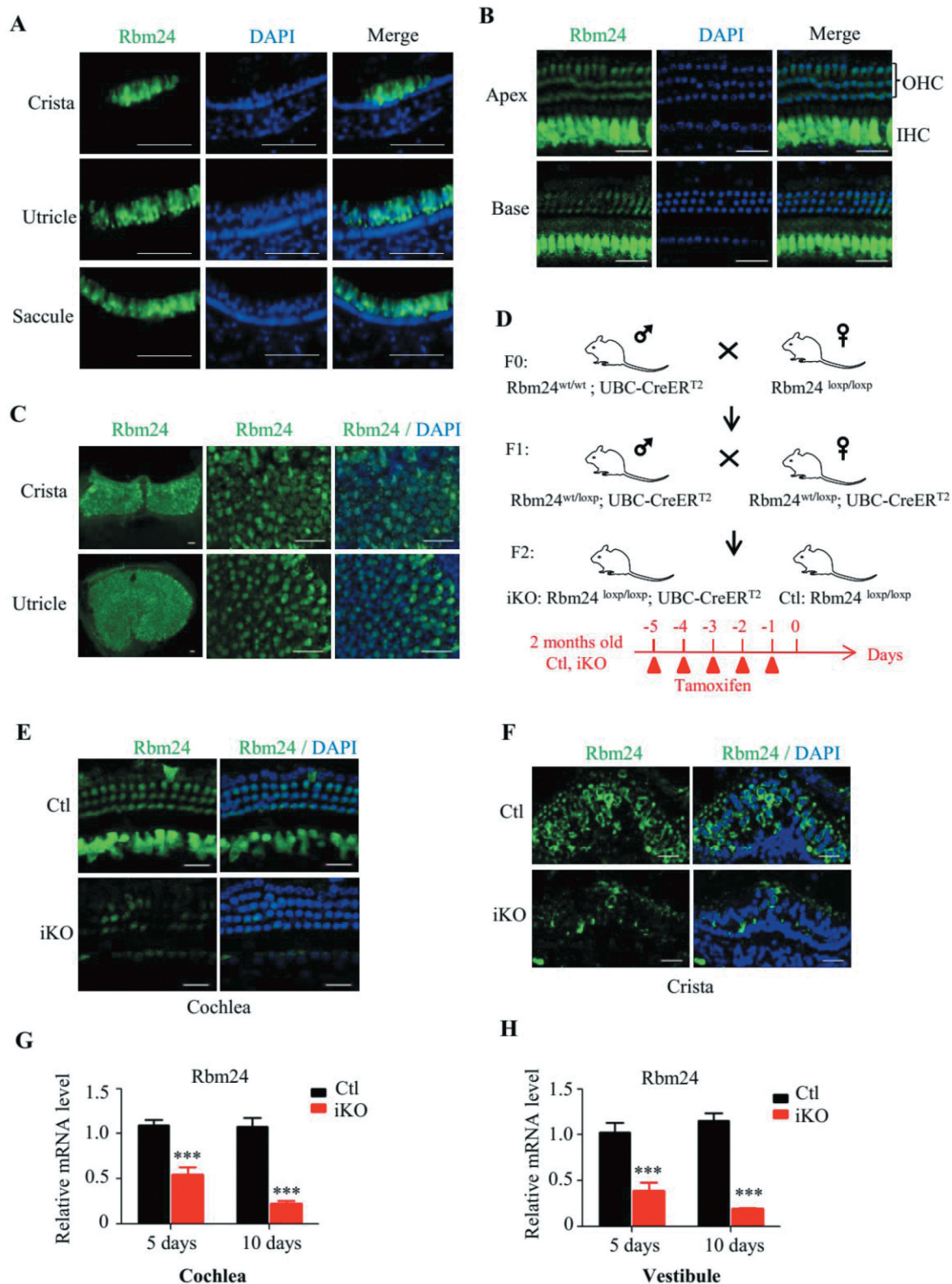
Figure 1. Rbm24-dependent AS transcripts are related to the integrity of stereocilia and the survival of hair cells.

(A) List of the genes alternatively spliced in response to loss of Rbm24 that are associated with the integrity of stereocilia and the survival of hair cells. (B) Schematic of the molecular structure of the stereocilia tip link apparatus based on Fettiplace *et al* [6]. (C) Schematic of the Atp2b2 molecular structure and its AS exons. Atp2b2 contains 10 TM domains, a PL domain and a CaM-BD. The AS sites at the CaM-BD are indicated below the model. The orange and green boxes represent Rbm24-dependent exons. The insert of Rbm24-dependent exons creates a new stop codon. RT-PCR was used to analyse Atp2b2 AS in the control and iKO inner ears and is shown under the model. The arrows indicate the primer positions. (D) Schematic of Kcnq4 AS exons. The orange box represents Rbm24-dependent exons. (E) RT-PCR analysis of Kcnq4 AS in control and iKO inner ears. Data are representative from 3–5 RNA samples. (F) Diagram of Kcnq4 splicing reporter construction strategy. (G) RT-PCR analysis of AS in HeLa cells transfected with the indicated plasmids. TM, transmembrane; PL, phospholipid sensitive; Cam-BD, calmodulin-binding domain.

Auditory brainstem response test

Prior to testing, mice were anaesthetized by injection of 100 mg/kg ketamine and 10 mg/kg xylazine. During the test, the mice were placed on a heating pad to maintain a constant body temperature. A loudspeaker was placed 10 cm away from the tested ear at a parallel height. Stimulation signals of click and tone bursts were generated by System 3 digital signal processing hardware and software (Tucker Davis Technologies, Florida, USA). Needle electrodes were inserted at the subcutaneous area of the vertex of the scalp, the post-auricular region (reference) and the back leg (ground) to record the response signals. Auditory thresholds were determined by decreasing the sound intensity of each stimulus from 90 dB SPL to 10 dB SPL in 10 dB steps until the lowest sound intensity with reproducible and recognizable waves in the response was reached. Thresholds were determined to within 5 dB by two researchers to ensure reliability [17].

Behaviour assays

Swimming test. The swimming test equipment used was a rectangular water tank with water kept at a normal temperature. The tank was 70 cm long, 40 cm wide and 10 cm deep. The mice were placed in the centre of the water tank, with their body parallel to the long axis of the water tank. The mouse's free swimming posture was observed by letting go of the mice. Scoring was performed as follows: 3, the mouse swam in a stable position with their heads above the water; 2, the mouse's head was out of the water, the swimming posture was unstable; 0, the mouse's head was not raised or above the surface of the water. The mice were rescued from the water immediately to avoid drowning [18,19].

Contact righting reflex. The mice were placed in a large glass petri dish that allowed them to move but with their feet and back in contact with the glass. Then, the dish was turned over to observe how the mice responded. The righting reflex was scored as follows: 3, mice turnover immediately (normal); 2, mice take several seconds to turnover (intermediate response); 0, mice failed to turnover (severe response) [19].

RT-PCR and qPCR

After 5 or 10 days following TMXF administration, the sensory organs of the inner ear were isolated for RNA extraction using Trizol® reagent (Invitrogen; Thermo Fisher Scientific, Inc., Waltham, MA, USA). RNA was extracted according to the manufacturer's protocol. A total of 1 μg of total RNA was used for cDNA synthesis by using SuperScript II reverse transcriptase kit [reaction mix contain Anchored Oligo(dT) 18 Primer and Random Primer(N9)] (TransGen Biotech; Cat. no. AE341, Peking, China). PCR amplification consisted of 25–32 cycles, followed by electrophoresis on high-resolution agarose gel to detect PCR products. qPCR was performed using an ABI7500 real-time PCR system (Thermo Fisher Scientific, Inc., Waltham, MA, USA). Primers for RT-PCR and qPCR are listed in Table S3.

RNA-seq

A total of 5 days after TMXF administration, vestibular sensory organs were collected for RNA extraction and used for high-throughput RNA sequencing (n = 3). Subsequently, generation of the sequencing library preparations were constructed according to the manufacturer's protocol (NEBNext® Ultra™ RNA Library Prep Kit for Illumina®; New England BioLabs, Inc., Ipswich, MA, USA). Sequencing was performed using a 2 × 150 bp paired-end (PE) configuration. Image analysis and base calling were conducted using the HiSeq Control Software (HCS) + OLB + GAPipeline-1.6 (Illumina, Inc.) on the HiSeq instrument. A total of three biological replicates from both the control and iKO mice were sequenced to a depth of 40–60 million reads. FASTQ files from the RNA-seq were processed using the FastQC tool (bioinformatics.bbsrc.ac.uk/projects/fastqc/) to obtain high quality clean data. Qualified clean data were mapped to the reference mouse genome (GRCm38/mm10) and splice junctions were identified using TopHat [20]. Transcript assembly and expression abundance analysis were analysed using Cufflinks [21]. ASprofile version 1.0 was used to extract, compare and classify AS events from the result of Cufflinks [21].

GO analysis

The mean FPKM of genes ≥ 4 and with a fold change ≥ 1.5 were selected for GO analysis (Table S2). AS events were selected with read counts of transcripts ≥ 50 in at least one sample and an absolute value of IncLevelDifference ≥ 1.5 (Table S1). GO analysis was performed using DAVID Bioinformatics Resources version 6.7 (david.abcc.ncifcrf.gov/). All genes in the mouse genome were used as the background control. The significance cut-off for P-value was set at 0.05.

Cell culture

HeLa and 293 FT cells were obtained from the Cell Resource Centre of the Chinese Academy of Sciences (Shanghai, China) and were maintained in DMEM (Thermo Fisher Scientific, Inc. Waltham, MA, USA) supplemented with 10% FBS (Thermo Fisher Scientific, Inc. Waltham, MA, USA) and 1% penicillin/streptomycin at 37°C with 5% CO_2 in a humidified incubator.

Construction of splicing reporters

Cdh23 AS fragments containing exon 67, intron 67, exon 68, intron 68 and exon 69 were amplified from mouse genome DNA. Fragment was then cloned into pXJ40-myc plasmids using the following restriction sites: HindIII and NotI. Rbm24 binding site deletions were achieved by overlap-extension PCR. Rbm24 overexpression plasmids were constructed by inserting the mouse Rbm24 coding sequence into the pXJ40 plasmids. Kcnq4 mini-splicing reporter (Kcnq4-mini) recapitulates splicing of the Kcnq4 genomic locus. Kcnq4 intron 11 was shortened internally. Kcnq4-

mini was assembled from 2 fragments: exon 8-intron 8-exon 9-intron 9-exon 10-intron 10-exon 11-intron 11 (fragment 1) and intron 11-exon 12 (fragment 2). Kcnq4 AS fragments were then cloned into pXJ40-myc plasmids using the following restriction sites: HindIII, XhoI and NotI. Reporter plasmids and Rbm24 overexpression plasmids were transfected into 293 FT or HeLa cells using PEI transfection reagent (Sigma-Aldrich; Merck KGaA-Aldrich; Merck KGaA). After 48 h, RNA was extracted and used for AS pattern examination. The sequences of the PCR primers used for splicing reporter construction are listed in Table S3.

Statistical analysis

Results are presented as mean ± standard error of the mean, and statistical significance was tested using two-tailed student's t-tests. Differences were considered significant at a value of $P < 0.05$.

Results

Rbm24 expression in the inner ear and generation of Rbm24 iKO mice

First, we examined Rbm24 expression in the inner ear. As shown in Fig. 1A, Rbm24 was strongly expressed in the inner ear hair cells of the vestibular sensory organs (including crista, saccula and utricle). The expression patterns observed were similar to a previous study [16], although we found that Rbm24 was only expressed in the hair cells, and not in the adjacent supporting cells. Next, we performed wholemount immunostaining on the different regions of the cochlear sensory organ of the corti. As shown in Fig. 1B, Rbm24 was expressed in both the inner hair cells (IHCs) and outer hair cells (OHCs) in different regions of corti, and the Rbm24 expression levels in IHCs was higher compared with OHCs. In addition, wholemount immunostaining of the vestibular sensory organ of the crista and utricle revealed that Rbm24 was expressed in the entirety of the sensory epithelium, wherein the vestibular Type I and Type II hair cells are located (Fig. 1C). We further analysed the subcellular localization of Rbm24 in inner ear hair cells and the results showed that Rbm24 was localized in both the nucleus and cytosol of crista hair cells, IHCs and OHCs, with relatively higher levels in the cytosol (Fig. S1).

To determine the functional involvement of Rbm24 in the inner ear and gain insight into the molecular basis of the phenotype, we generated Rbm24 iKO mice (Figs 1D and S2). Mice carrying the conditional Rbm24 allele (Rbm24$^{loxp/loxp}$) [14] were crossed to a transgenic line UBC-CreER^{T2}, in which the recombinase activity is activated by TMXF, to generate the Rbm24 iKO mice (CreER^{T2}-Rbm24$^{loxp/loxp}$). Rbm24 knockout was induced by TMXF administration in 2 months old mice for 5 days (Fig. 1D). After TMXF treatment, cortis and cristae were dissected to analyse the Rbm24 knockout efficiency. Wholemount immunostaining of cortis and cristae showed that the expression of Rbm24 was decreased in the majority of hair cells (Fig. 1E,F). Quantitative-PCR (qPCR) analysis showed that expression of Rbm24 was downregulated ~50% in the iKO mice 5 days after TMXF administration, and downregulated by 80% 10 days after TMXF administration (Fig. 1G,H).

Rbm24 deletion results in hearing loss and motor coordination defects

The inner ear is a structurally complex vertebrate organ that is essential for hearing and motor coordination in mice [5]. Inner ear dysfunction results in hearing loss and disequilibrium (characteristics include circling and head bobbing) in mice [22]. At ~1 month after TMXF administration, we evaluated the hearing of iKO mice and found mice were notably deaf. By using the click-ABR test, iKO mice failed to elicit any waveforms, even under the maximum stimulation levels (Fig. 2A). In addition, the tone burst-ABR test revealed that their hearing was lost at all tested frequencies (Fig. 2B). Furthermore, mice exhibited head bobbing, circling and orientation defective behaviours, the typical characteristics of severe vestibular dysfunction [23] (Video S1). Thus, contact righting reflex was tested, which requires a combination of visual, vestibular and somatosensory inputs to make postural adjustments following displacement [24]. When iKO mice were placed on their backs, they completely failed to adjust themselves (Fig. 2C and Video S1). Next, we performed swimming analysis by placing mice in a water tank. iKO mice rolled up and down, indicating that they suffered from a severe motor coordination defect (Fig. 2D and Video S1). These data suggest that Rbm24 was essential for maintaining auditory and motor coordination function in the inner ear.

Rbm24 deletion results in hair cell degeneration, stereocilia loss and disorganization

At ~1 month after Rbm24 deletion, ~40% of the OHCs were lost, and the loss of OHCs continued to increase over time (70% after 3 months later) (Fig. 3A,B). However, the number of IHCs was not altered (Fig. 3A,B), even though the Rbm24 expression level in IHCs was higher compared with OHCs (Fig. 1B). We then investigated the stereocilia of cochlea hair cells and found that the stereocilia of both IHCs and OHCs were either lost or were present in a notably disorganized manner (Figs 3C and S3), and the severity of stereocilia loss increased over time (Fig. 3C). Similarly, in the vestibular utricle and crista, the stereocilia were also notably lost, and the loss of stereocilia became more severe over time (Fig. 3D, E). In addition, the number of utricle hair cells was reduced (Fig. 3F) although the reduction was small. In summary, these results suggest that Rbm24 is essential for the survival of hair cells and the integrity of stereocilia. The hearing loss and motor coordination defects observed in iKO mice were primarily attributed to hair cell degeneration and stereocilia loss.

Rbm24 regulates AS in the inner ear

To investigate whether Rbm24 regulates AS in the inner ear, we analysed the transcriptome of the vestibular sensory organs in the control and Rbm24 deletion groups using RNA sequencing
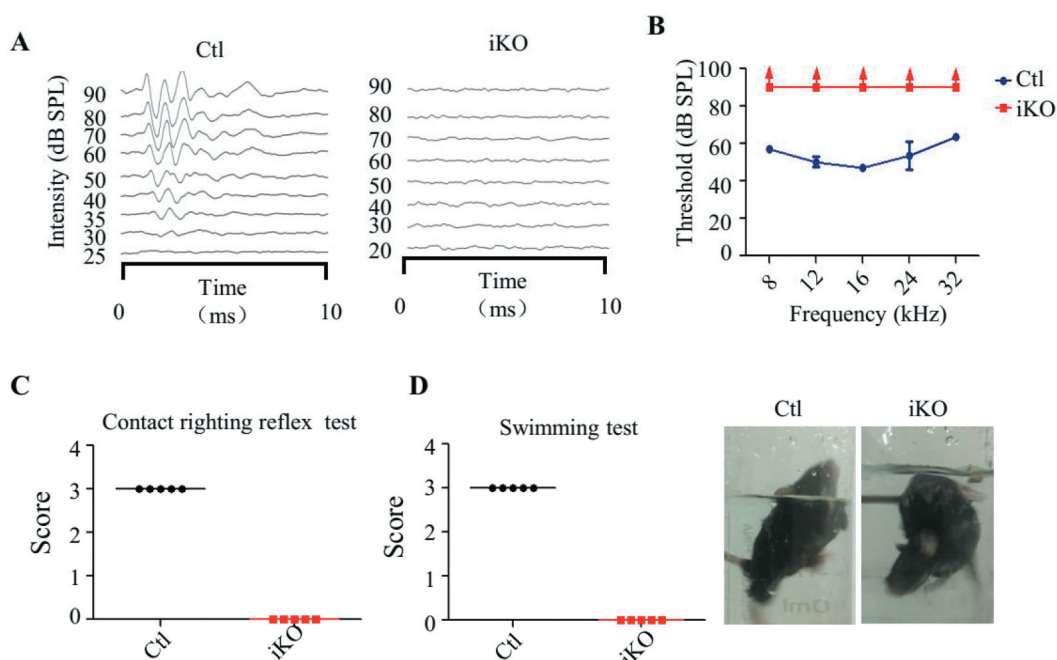
Figure 2. Rbm24 deletion resulted in motor coordination defects and hearing loss.

(A) The ABR click test showed that iKO mice failed to elicit waveforms even under maximum stimulation, indicating that iKO mice were completely deaf (n = 3). (B) The ABR pure tone-burst test showed iKO mice were notably deaf at all tested frequencies (n = 3). Red arrows on the symbols indicate the maximum sound pressure level tested. (C) Contact righting reflex tests showed iKO mice failed to adjust themselves, indicating that vestibular function was impaired (n = 5). (D) The swimming test showed that control mice swam in the water, while iKO mice rolled up and down in the water (n = 5). Data are presented as the mean ± standard error of the mean. ABR, auditory brainstem response.

(RNA-seq; n = 3). In aggregate, we identified 425 altered splicing events that belonged to 386 genes, and these could be classified into five basic AS modes: Skipped exons (SE), mutually exclusion exons (MXE), alternative 5′ splice sites (A5SS), alternative 3′ splice sites (A3SS), and retained introns (RI) (Fig. 4A and Table S1). Interestingly, about half of the altered splicing belonged to the SE type and most of them were exon exclusion (Fig. 4B), suggesting that Rbm24 acts primarily as a splicing repressor in the inner ear, similar to its function in the heart [12,14]. In the total of 386 genes that were identified to be potentially regulated by Rbm24 in this analysis, there were some AS events that had previously been reported to be responsive to Rbm24, such as Ndrg4, Etv6, Agap1, Immt and Synj2 [14]. We further validated seven AS events using RT-PCR. As shown in Fig. S4, deletion of Rbm24 changed the isoform patterns of each detected transcript, suggesting high confidence in our RNA-seq analysis.

In order to obtain a functional overview of the genes whose pre-mRNA were differentially spliced, we performed gene ontology (GO) analysis using DAVID (david.ncifcrf.gov/). As shown by biological process analysis, Rbm24-regulated AS transcripts encoding proteins were significantly enriched in the process involved in the functionality of inner ear, such as, sensory perception of sound, equilibrioception, inner ear development and auditory receptor cell differentiation. (Fig. 4C). Furthermore, cellular component analysis revealed that a panel of Rbm24-regulated splicing transcripts encoding proteins were localized in the stereocilia tip (Fig. 4D), suggesting that Rbm24-dependent AS may be involved in regulating stereocilia organization.

Importantly, we identified a group of Rbm24-regulated inner-ear-specific exons (Fig. 4E,F). These Rbm24-dependent inner-ear-specific exons are derived from genes involved in hearing loss and motor coordination disorders in humans and mice; examples of which include Ush1c [25], Myo7a [26], Pcdh15 [27], Cdh23 [28], Cacna1d [29], Ptprq [30] and Atp2b2 [31]. Through splicing assay, we observed a dramatic reduction in the inclusion of inner-ear-specific exons in Rbm24 deletion in the inner ears (Fig. 4E), suggesting that Rbm24 may be a major regulator of these exons. Analysis of these Rbm24-regulated exons in different mouse tissues showed that most of these exons were specifically enriched in the inner ear (Fig. 4F). Intriguingly, although Cdh23, Myo7a and Ush1c are abundantly expressed in both the inner ear and striated muscle, the Rbm24-regulated splicing isoform of these genes were only present in inner ear and not in striated muscle (Fig. 4E,F), indicating that splicing regulation of these genes was tissue-specific.

In addition, we also analysed the gene expression networks that were disrupted in the iKO mice. Our analysis revealed 275 genes (179 downregulated and 96 upregulated) that were differentially expressed between control and iKO mice (fold change ≥ 1.5, P < 0.05, Fig. S5A and Table S2). In order to obtain a functional overview of the genes that were differentially expressed in the iKO mice, we grouped the differentially expressed genes into GO categories using DAVID. GO analysis of differentially expressed genes indicated that they were enriched in the adult walking behaviour, synapse, syntaxin-1 binding and SNARE complex (such as Snap25, Cplx1) (Fig. S5B, C and D). We further verified the expression levels of
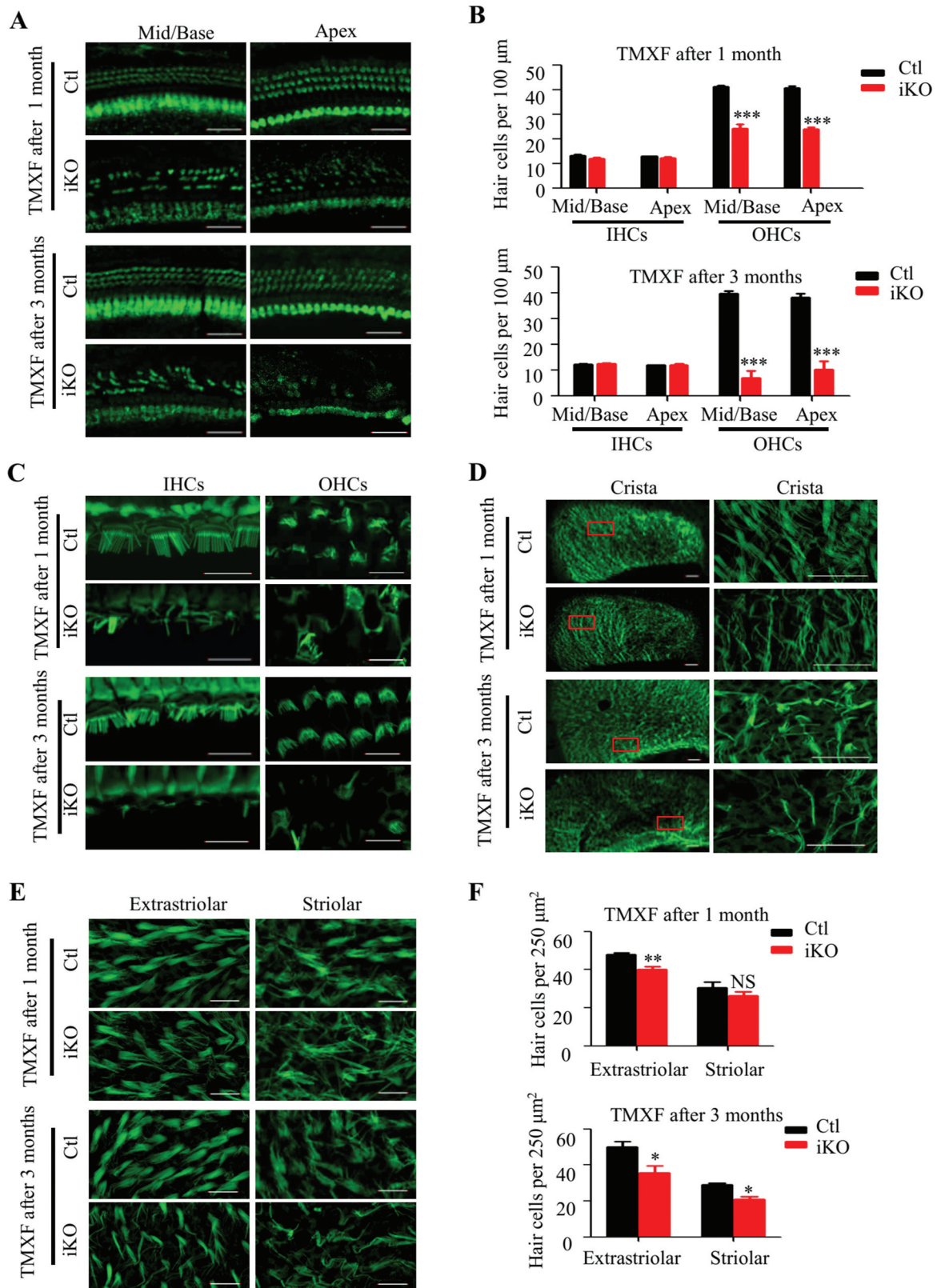
Figure 3. Rbm24 deletion results in hair cell degeneration, or loss and disorganization of stereocilia.

(A and B) Wholemount immunostaining of a cochlea with the hair cell marker gene myo7a 1 and 3 months after TMXF administration. About 40% of the OHCs were lost, and the severity of the loss increased with time (70% after 3 months), while the number of IHCs did not change. The number of IHCs and OHCs was quantified, respectively, and are shown in (B) (n ≥ 3). Scale bar, 40 μm. (C) Phalloidin staining of wholemount cochlea. The stereocilia of both the IHCs and OHCs were notably lost, or were present in a notably disorganized manner, and the severity increased over time (n ≥ 3). Scale bar, 10 μm. (D) Phalloidin staining of wholemount crista. Stereocilia were notably lost 1 month after TMXF administration, and the severity increased over time (n = 3). The right row shows higher magnification versions of the images on the left marked by the red box. Scale bar, 20 μm. (E and F) Phalloidin staining of a whole-mount utricle. The stereocilia of utrical hair cells were slightly lost 1 month after TMXF administration, and the loss became more prominent over time. The number of hair cells was counted and quantified according to the number of hair bundles, and is shown in graph F (n ≥ 4). Scale bar, 10 μm. Data are presented as the mean ± standard error of the mean. *$P < 0.05$, **$P < 0.01$, ***$P < 0.0001$. NS, not significant.
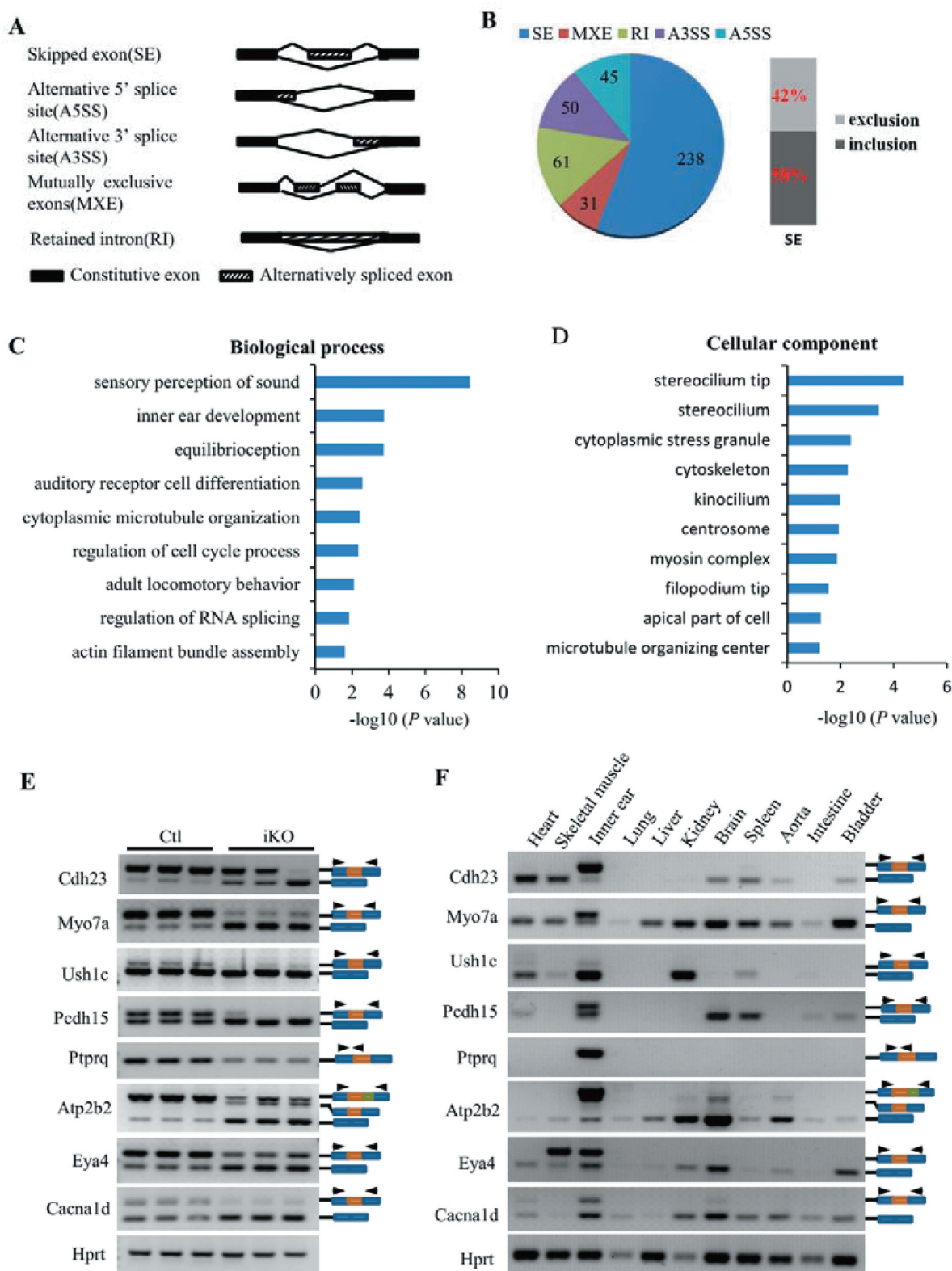
Figure 4. Rbm24 regulates AS in the inner ear.
(A) Diagram of AS patterns regulated by Rbm24. (B) The proportion of AS types in response to Rbm24 deletion. (C and D) GO analysis of the genes alterenatively spliced in response to loss of Rbm24. (E) RT-PCR analysis of Rbm24-dependent splicing in control and iKO inner ears. (F) RT-PCR analysis of Rbm24-dependent splicing in different adult mice tissues. The arrows indicate the primer positions. The orange boxes represent Rbm24-dependent exons. Hprt was used as the internal control. AS, alternative splicing; GO, Gene Ontology.

Snap25 and Cplx1 by qPCR and found they were downregulated in the iKO mice (Fig. S5E). These data suggested that Rbm24 deletion may also affect the synaptic signal transmission of hair cells.

Misregulated splicing of inner-ear-specific exons is related to the integrity of stereocilia and the survival of hair cells

As verified in Fig. 4E,F, we identified a group of Rbm24-regulated inner-ear-specific exons. Through detailed analysis, we found that many of these were derived from genes related to stereocilia (Fig. 5A), such as Ush1c [25], Myo7a [26], Cdh23 [28], Pcdh15 [27] and Ptprq [32]. Cdh23 and Pcdh15 are components of the stereocilia tip link and interact with each other between the adjacent stereocilia [33]; unconventional myosin Myo7a and adaptor protein Ush1c interact with Cdh23 and form a ternary complex at the upper part of the tip link [34] (Fig. 5B). The AS changes of these transcripts in Rbm24 deficient inner ears may affect the assembly of the tip link, leading to the disorganization of stereocilia. In addition, we identified Rbm24-regulated splicing of a plasma membrane calcium ATPase, Atp2b2, which serves important roles in maintaining stereocilia integrity and the survival of hair cells by extrusion of Ca^{2+} from the stereocilia to the endolymph (Fig. 5B) [31,35]. At splice site C of Atp2b2 (localized in the calmodulin-binding domain), the insert of two alternative exons creates a novel stop codon, leading to the truncation of the pump (variant A) (Fig. 5C), which exhibits increased basal Ca^{2+} extrusion activity and is essential to meet the special Ca^{2+} homoeostasis demands of the endolymph and of the stereocilia [36]. Rbm24 deletion significantly reduced the expression of variant A, which may affect the function of Atp2b2, leading to the disorganization and loss of stereocilia, and thus the degeneration of hair cells.

In addition to Atp2b2, we also identified a panel of Rbm24-regulated splicing transcripts encoding proteins related to the survival of hair cells, such as inositol lipid phosphatase Ptprq [32], transcriptional co-activator Eya4 [37], L-type voltage-dependent Ca^{2+} channel Cacna1d [38] and voltage-gated potassium channel Kcnq4 [39]. Among these genes, we found that Kcnq4 dysfunction resulted in degeneration of OHC, rather than IHC [39], similar to the gradual degeneration of OHCs in our Rbm24 iKO mice (Fig. 3A). In the cochlea, four AS variants of Kcnq4 have been identified (Fig. 5D), which differ in the use of exon 9–11 and exhibit distinct voltage-dependent and calmodulin-binding properties [40,41]. The random heteromerization of different Kcnq4 splicing variants and their functional interactions with other Kcnq channels are characteristic of the functional diversity of Kcnq4 [41]. In this study, we showed that Rbm24 deletion disrupted the splicing pattern of Kcnq4, and the V3 isoform almost disappeared in both the cochlea and vestibule (Fig. 5E), indicating that Kcnq4 potassium transport function may be impaired. However, only V1 and V3 variants were detected in the wild-type vestibule and cochlea at this time point, which may be due to alterations of the expression of different Kcnq4 variants during development [40]. In addition, we confirmed that Rbm24 was a direct splicing regulator

of Kcnq4 by performing a splicing reporter assay. We constructed a Kcnq4 splicing mini gene's expression plasmid (Fig. 5F) and transfected it with Rbm24 into HeLa cells. We found that exogenously expressed Rbm24 in HeLa cells promoted the expression of Kcnq4 variant 3 (Fig. 5G), indicating Rbm24 directly regulates the splicing of Kcnq4.

Rbm24 directly regulates the inner-ear-specific splicing of Cdh23

Cdh23 is a component of tip links and serves an important role in regulating the morphology of stereocilia [28]. Mutations in Cdh23 result in human Usher syndrome type 1D congenital hearing loss [42]. Specifically, the cytoplasmic domain of Cdh23 contains an AS exon, known as the 68th exon of Cdh23, which is only included in the mRNA expressed in the inner ear (Fig. 6A) [42]. The inclusion of exon 68 has been suggested to affect the conformation as well as protein–protein interactions of Cdh23 [43,44]. As shown in Fig. 4E, we found that Rbm24-regulated AS of Cdh23. So we further analysed the altered exon and confirmed that it was exon 68 of Cdh23 that was alternatively spliced by Rbm24. In both the cochlea and vestibule, Rbm24 promoted the inclusion of this exon (Fig. 6B). In order to study the splicing mechanism of this exon, we constructed a Cdh23 splicing reporter (Fig. 6C). When we co-transfected this reporter with Rbm24 into 293 FT or HeLa cells, we found that Rbm24 dramatically induced the inclusion of exon 68 (Fig. 6D), indicating that Rbm24 was sufficient to drive the AS of Cdh23 as a tissue-specific splicing factor, even in non-hair cells. Furthermore, we identified that there were two Rbm24-binding motifs (GT rich sequences) [12,14] downstream of exon 68 (Fig. 6E). When we deleted either or both of these, the inclusion efficiency was notably reduced, suggesting that both GT stretches downstream of exon 68 are required for the inclusion of exon 68 (Fig. 6F). In conclusion, these data suggest that Rbm24 is a direct splicing regulator of Cdh23 exon 68, and Rbm24 is able to drive the AS of Cdh23 in inner ear and non-hair cells, and this splicing evidently does not rely on a tissue-specific cofactor.

Discussion

Cell-type-specific splicing serves an important role in organ development and disease manifestation [12], while little is known about the factors and mechanisms directing inner-ear-specific splicing. In the present study, we systematically analysed the function of a tissue-specific splicing factor, Rbm24, in the inner ear, and found > 400 misregulated AS events in response to Rbm24 deficiency (Fig. 4B). Rbm24 deletion resulted in degeneration of OHCs, and loss or disorganization of stereocilia, which in-turn resulted in hearing loss and motor coordination defects in mice.

We found that Rbm24 was highly expressed in the inner ear hair cells and regulated the inclusion of several inner-ear-specific exons. Loss of function of Rbm24 was shown to alter AS of pre-mRNAs involved in regulating the functions of the inner ear, such as the stereocilium morphogenesis-related genes Cdh23, Myo7a, Pcdh15 and Atp2b2 (Fig. 4E). Rbm24
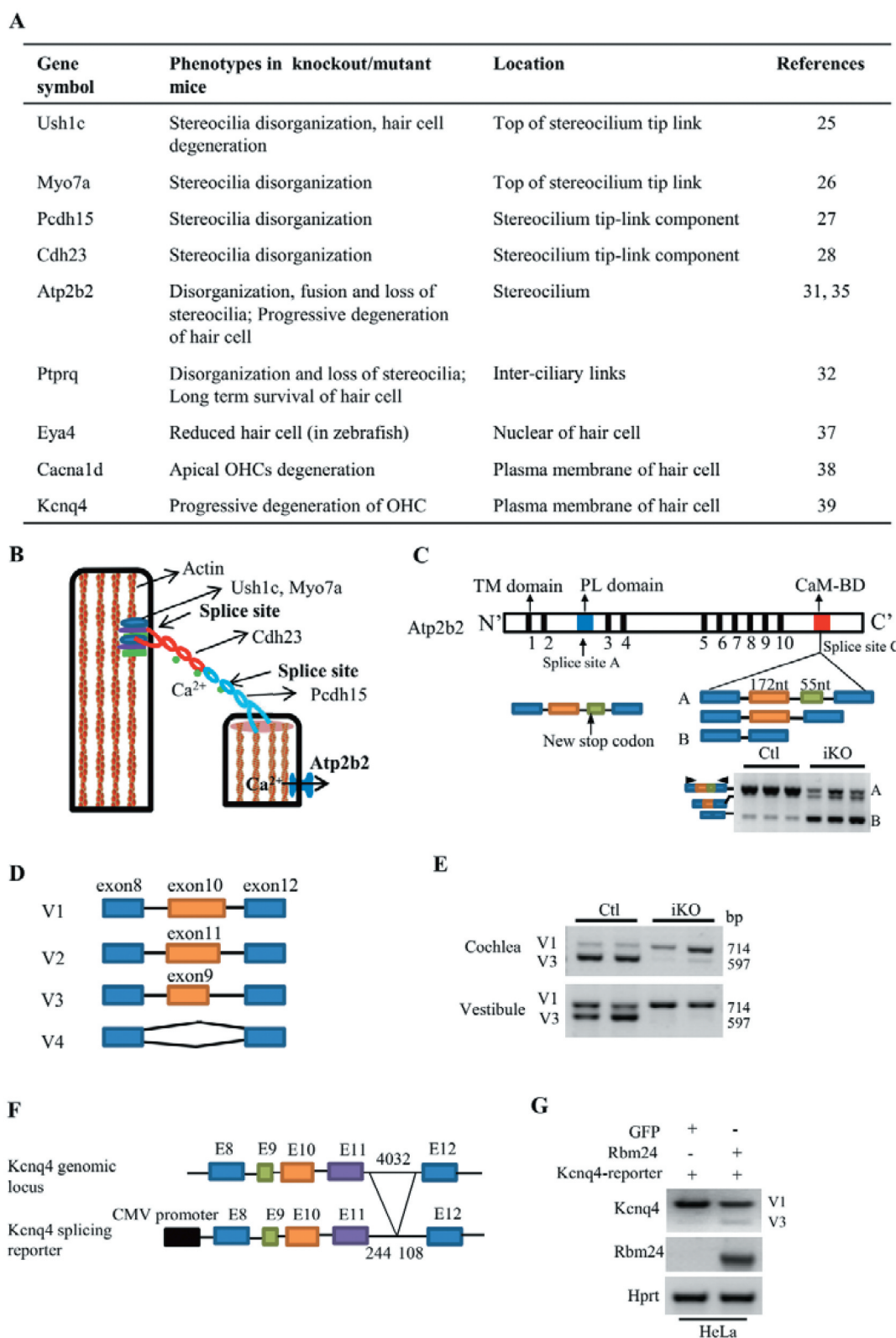
Figure 5. Rbm24-dependent AS transcripts are related to the integrity of stereocilia and the survival of hair cells.

(A) List of the genes alternatively spliced in response to loss of Rbm24 that are associated with the integrity of stereocilia and the survival of hair cells. (B) Schematic of the molecular structure of the stereocilia tip link apparatus based on Fettiplace et al (6). (C) Schematic of the Atp2b2 molecular structure and its AS exons. Atp2b2 contains 10 TM domains, a PL domain and a CaM-BD. The AS sites at the CaM-BD are indicated below the model. The orange and green boxes represent Rbm24-dependent exons. The insert of Rbm24-dependent exons creates a new stop codon. RT-PCR was used to analyze Atp2b2 AS in the control and iKO inner ears and is shown under the model. The arrows indicate the primer positions. (D) Schematic of Kcnq4 AS exons. The orange box represents Rbm24-dependent exons. (E) RT-PCR analysis of Kcnq4 AS in control and iKO inner ears. Data are representative from 3–5 RNA samples. (F) Diagram of Kcnq4 splicing reporter construction strategy. (G) RT-PCR analysis of AS in HeLa cells transfected with the indicated plasmids. TM, transmembrane; PL, phospholipid sensitive; Cam-BD, calmodulin binding domain.
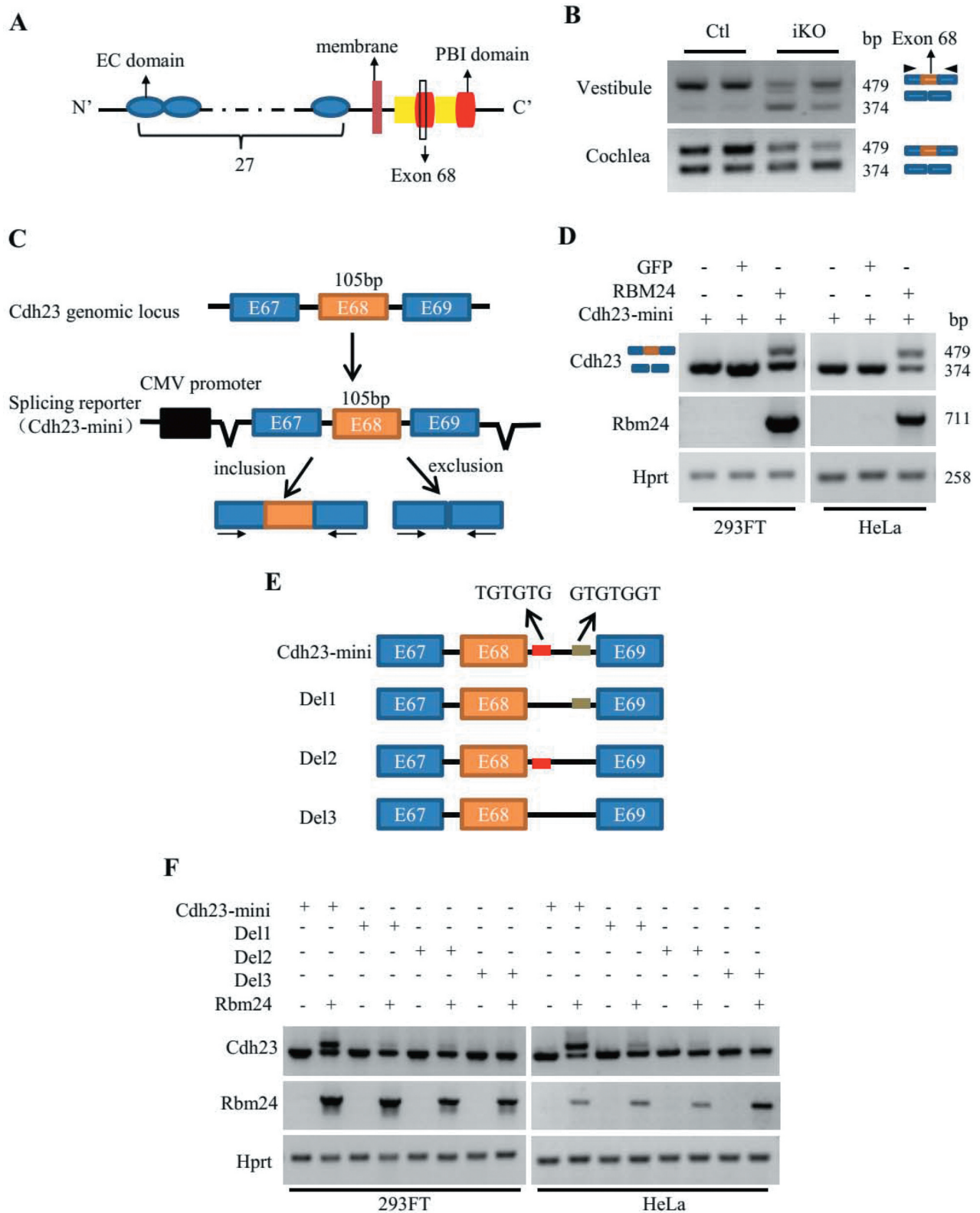
Figure 6. Rbm24 directly regulates the splicing of Cdh23 inner-ear-specific exons.

(A) Schematic of the Cdh23 molecular structure. Cdh23 contains 27 EC domains, a single pass trans-membrane domain and a cytoplasmic domain. The AS exon (exon 68) is located in the PBI. (B) RT-PCR analysis of the splicing of Cdh23 exon 68 in the vestibule and cochlea. Data are representative from 4–6 RNA samples. (C) Cdh23 splicing reporter construction diagram. A splicing fragment containing exons 67, 68, and 69, and introns 67 and 68, was inserted into a Pxj40 plasmid. (D) RT-PCR analysis of AS in 293 FT and HeLa cells transfected with the indicated plasmids. (E) Schematic of the Cdh23 splicing fragment. Two clusters of Rbm24 binding sites (GT enrichment sequence) were found in intron 68. Either or both GT stretches were deleted from the Cdh23-mini reporter. (F) RT-PCR analysis of RNA splicing in HeLa and 293 FT cells transfected with the indicated plasmids. EC, extracellular cadherin; PBI, PDZ binding interface.

deletion significantly decreased the inclusion of these inner-ear-specific exons, and we found that exogenously expressed Rbm24 in 293 FT and HeLa cells induced the inclusion of exon 68 of Cdh23 (Fig. 6), indicating that Rbm24 may be a direct AS regulator of these inner-ear-specific exons. Interestingly, we found that two clusters of GU stretches localized downstream of exon 68 of Cdh23 are required for the inclusion of this exon. The GU-rich stretches were also found in other transcripts regulated by Rbm24, such as Naca and Titin [12,14]. While in Titin, the GU stretches flank on the up- and down-stream of spliced exon [14]. These data suggest that while a GU-rich sequence is required for Rbm24 binding, the position of the GU stretch may not affect the regulated exons.

Previous studies demonstrated that Rbm24 was highly expressed in striated muscles and regulated a number of AS events in the heart [12,14]. Therefore, we compared the genes whose pre-mRNA were differentially spliced between the heart and inner ear and found little overlap (Fig. S6 and Table S1), suggesting that Rbm24 regulated different AS transcripts in different tissues. For example, certain Rbm24-dependent exons were only present in the inner ear, such as Cdh23 exon 68. As demonstrated in Fig. 6, Rbm24 was able to drive the inclusion of this tissue-specific exon, even in another type of human cell unrelated to ears. However, this exon is skipped in heart (Fig. 4F). As indicated in previous study [12], the balance between splicing repressors and activators serves a critical role in controlling splicing. We hypothesized that there may exist differences in the balance between splicing activators and repressors which may explain why the splicing pattern of a single exon is different between the heart and inner ear. As for the 23 genes commonly regulated by Rbm24 in both tissues, they are likely downstream targets directly regulated by Rbm24 regardless of the tissue background.

In Rbm24 iKO mice, we found that the mice were deaf and exhibited severe motor coordination defects, characteristic of severe vestibular dysfunction. Even though Rbm24 was highly expressed in the striated muscle, we did not observe any abnormal behaviour in the Rbm24 heart-specific knockout mice [14], indicating that these phenotypes are not caused by striated muscle dysfunction. As validated in Fig. 3, the inner ear hair cells and the stereocilia were severely degenerated, and led to dysfunction of the inner ear, which may be primarily responsible for the resultant hearing loss and motor coordination defects in the iKO mice.

To date, only one AS factor, Srrm4, has been shown to regulate AS in the inner ear, to the best of our knowledge [4,45]. Srrm4 requires GC motifs near the 3′ ends of the polypyrimidine tracts for exon inclusion [45], while Rbm24 requires GU motifs for exon inclusion, indicating that they regulate different panels of AS events in the inner ear. In Srrm4 mutant mice, the IHCs, but not the OHCs were degenerated [45], in contrast to the OHC degeneration observed in the Rbm24 iKO mice. However, in both Rbm24- and Srrm4-deficient mice, the stereocilia were lost, suggesting that the molecular network of stereocilia was impaired in both the Rbm24 and Srrm4-deficient mice. A considerable number of genes undergo complex AS in the inner ear, and therefore, these two AS factors may only be the tip of the iceberg, and a large amount of studies are still required to improve our understanding of the AS mechanisms of the inner ear.

At present, it is suggested that >90% of human multiexon genes are alternatively spliced [12], and the mutations that inhibit splicing of exons have been shown to associated with inherited hearing loss, such as SRRM4 dependent AS exon of REST [46]. In humans, inhibition of the frameshifting splicing events by a REST variant is associated with dominantly inherited deafness, highlighting the importance of AS regulation for hearing in humans [46]. It will be of great interest to determine whether the mutation(s) in Rbm24 are associated with hearing loss in humans.

Availability of data

RNA-seq data were uploaded to the NCBI's BioProject database under accession number PRJNA641557.

Disclosure statement

No potential conflict of interest was reported by the authors.

ORCID

Xiu Qin Xu http://orcid.org/0000-0003-3720-5088

References

[1] Motavaf M, Soveizi M, Maleki M, et al. MYO15A splicing mutations in hearing loss: A review literature and report of a novel mutation. Int J Pediatr Otorhinolaryngol. 2017;96:35–38.

[2] Morton CC, Nance WE. Newborn hearing screening–a silent revolution. N Engl J Med. 2006;354(20):2151–2164.

[3] Kremer H. Hereditary hearing loss; about the known and the unknown. Hear Res. 2019;376:58–68.

[4] Wang Y, Liu Y, Nie H, et al. Alternative splicing of inner-ear-expressed genes. Front Med. 2016;10(3):250–257.

[5] Wu DK, Kelley MW. Molecular mechanisms of inner ear development. Cold Spring Harb Perspect Biol. 2012;4(8):a008409.

[6] Fettiplace R. Hair cell transduction, tuning, and synaptic transmission in the mammalian cochlea. Compr Physiol. 2017;7 (4):1197–1227.

[7] OM D, Ricci AJ. A bundle of mechanisms: inner-ear hair-cell mechanotransduction. Trends Neurosci. 2019;42(3):221–236.

[8] Geleoc GS, Holt JR. Sound strategies for hearing restoration. Science. 2014;344(6184):1241062.

[9] Velez-Ortega AC, Frolenkov GI. Building and repairing the stereocilia cytoskeleton in mammalian auditory hair cells. Hear Res. 2019;376:47–57.

[10] Xu XQ, Soo SY, Sun W, et al. Global expression profile of highly enriched cardiomyocytes derived from human embryonic stem cells. Stem Cells. 2009;27(9):2163–2174.

[11] Poon KL, Tan KT, Wei YY, et al. RNA-binding protein RBM24 is required for sarcomere assembly and heart contractility. Cardiovasc Res. 2012;94(3):418–427.

[12] Yang J, Hung LH, Licht T, et al. RBM24 is a major regulator of muscle-specific alternative splicing. Dev Cell. 2014;31(1):87–99.

[13] Zhang T, Lin Y, Liu J, et al. Rbm24 regulates alternative splicing switch in embryonic stem cell cardiac lineage differentiation. Stem Cells. 2016;34(7):1776–1789.

[14] Liu J, Kong X, Zhang M, et al. RNA binding protein 24 deletion disrupts global alternative splicing and causes dilated cardiomyopathy. Protein Cell. 2019;10(6):405–416.

[15] Grifone R, Xie X, Bourgeois A, et al. The RNA-binding protein Rbm24 is transiently expressed in myoblasts and is required for myogenic differentiation during vertebrate development. Mech Dev. 2014;134:1–15.

[16] Grifone R, Saquet A, Xu Z, et al. Expression patterns of Rbm24 in lens, nasal epithelium, and inner ear during mouse embryonic development. Dev Dyn. 2018;247(10):1160–1169.

[17] Xie WR, Jen HI, Seymour ML, et al. An Atoh1-S193A phospho-mutant allele causes hearing deficits and motor impairment. J Neurosci. 2017;37(36):8583–8594.

[18] Dong S, Leung KK, Pelling AL, et al. Circling, deafness, and yellow coat displayed by yellow submarine (ysb) and light coat and circling (lcc) mice with mutations on chromosome 3. Genomics. 2002;79(6):777–784.

[19] Al Deeb S, Al Moutaery K, Khan HA, et al. Exacerbation of iminodipropionitrile-induced behavioral toxicity, oxidative stress, and vestibular hair cell degeneration by gentamicin in rats. Neurotoxicol Teratol. 2000;22(2):213–220.

[20] Kim D, Pertea G, Trapnell C, et al. TopHat2: accurate alignment of transcriptomes in the presence of insertions, deletions and gene fusions. Genome Biol. 2013;14(4):R36.

[21] Trapnell C, Williams BA, Pertea G, et al. Transcript assembly and quantification by RNA-Seq reveals unannotated transcripts and isoform switching during cell differentiation. Nat Biotechnol. 2010;28(5):511–515.

[22] Cryns K, van Alphen AM, van Spaendonck MP, et al. Circling behavior in the Ecl mouse is caused by lateral semicircular canal defects. J Comp Neurol. 2004;468(4):587–595.

[23] Deol MS. The anatomy and development of the mutants pirouette, shaker-1 and waltzer in the mouse. Proc R Soc Lond B Biol Sci. 1956;145(919):206–213.

[24] Ebrahim S, Ingham NJ, Lewis MA, et al. Alternative splice forms influence functions of whirlin in mechanosensory hair cell stereocilia. Cell Rep. 2016;15(5):935–943.

[25] Johnson KR, Gagnon LH, Webb LS, et al. Mouse models of USH1C and DFNB18: phenotypic and molecular analyses of two new spontaneous mutations of the Ush1c gene. Hum Mol Genet. 2003;12(23):3075–3086.

[26] Holme RH, Steel KP. Stereocilia defects in waltzer (Cdh23), shaker1 (Myo7a) and double waltzer/shaker1 mutant mice. Hear Res. 2002;169(1–2):13–23.

[27] Pawlowski KS, Kikkawa YS, Wright CG, et al. Progression of inner ear pathology in Ames waltzer mice and the role of protocadherin 15 in hair cell development. J Assoc Res Otolaryngology. 2006;7(2):83–94.

[28] Di Palma F, Holme RH, Bryda EC, et al. Mutations in Cdh23, encoding a new type of cadherin, cause stereocilia disorganization in waltzer, the mouse model for Usher syndrome type 1D. Nat Genet. 2001;27(1):103–107.

[29] Liaqat K, Schrauwen I, Raza SI, et al. Identification of CACNA1D variants associated with sinoatrial node dysfunction and deafness in additional Pakistani families reveals a clinical significance. J Hum Genet. 2019;64(2):153–160.

[30] Goodyear RJ, Jones SM, Sharifi L, et al. Hair bundle defects and loss of function in the vestibular end organs of mice lacking the receptor-like inositol lipid phosphatase PTPRQ. J Neurosci. 2012;32(8):2762–2772.

[31] Watson CJ, Tempel BL. A new Atp2b2 deafwaddler allele, dfw(i5), interacts strongly with Cdh23 and other auditory modifiers. Hear Res. 2013;304:41–48.

[32] Goodyear RJ, Legan PK, Wright MB, et al. A receptor-like inositol lipid phosphatase is required for the maturation of developing cochlear hair bundles. J Neurosci. 2003;23(27):9208–9219.

[33] Sakaguchi H, Tokita J, Muller U, et al. Tip links in hair cells: molecular composition and role in hearing loss. Curr Opin Otolaryngol Head Neck Surg. 2009;17(5):388–393.

[34] Bahloul A, Michel V, Hardelin JP, et al. Cadherin-23, myosin VIIa and harmonin, encoded by Usher syndrome type I genes, form a ternary complex and interact with membrane phospholipids. Hum Mol Genet. 2010;19(18):3557–3565.

[35] Bortolozzi M, Brini M, Parkinson N, et al. The novel PMCA2 pump mutation Tommy impairs cytosolic calcium clearance in hair cells and links to deafness in mice. J Biol Chem. 2010;285(48):37693–37703.

[36] Ficarella R, Di Leva F, Bortolozzi M, et al. A functional study of plasma-membrane calcium-pump isoform 2 mutants causing digenic deafness. Proc Natl Acad Sci U S A. 2007;104(5):1516–1521.

[37] Wang L, Sewell WF, Kim SD, et al. Eya4 regulation of Na+/K+-ATPase is required for sensory system development in zebrafish. Development. 2008;135(20):3425–3434.

[38] Dou H, Vazquez AE, Namkung Y, et al. Null mutation of alpha1D Ca2+ channel gene results in deafness but no vestibular defect in mice. J Assoc Res Otolaryngology. 2004;5(2):215–226.

[39] Kharkovets T, Dedek K, Maier H, et al. Mice with altered KCNQ4 K+ channels implicate sensory outer hair cells in human progressive deafness. Embo J. 2006;25(3):642–652.

[40] Beisel KW, Rocha-Sanchez SM, Morris KA, et al. Differential expression of KCNQ4 in inner hair cells and sensory neurons is the basis of progressive high-frequency hearing loss. J Neurosci. 2005;25(40):9285–9293.

[41] Xu T, Nie L, Zhang Y, et al. Roles of alternative splicing in the functional properties of inner ear-specific KCNQ4 channels. J Biol Chem. 2007;282(33):23899–23909.

[42] Vanniya SP, Srisailapathy CRS, Kunka Mohanram R. The tip link protein Cadherin-23: from hearing loss to cancer. Pharmacol Res. 2018;130:25–35.

[43] Yonezawa S, Hanai A, Mutoh N, et al. Redox-dependent structural ambivalence of the cytoplasmic domain in the inner ear-specific cadherin 23 isoform. Biochem Biophys Res Commun. 2008;366(1):92–97.

[44] Siemens J, Kazmierczak P, Reynolds A, et al. The Usher syndrome proteins cadherin 23 and harmonin form a complex by means of PDZ-domain interactions. Proc Natl Acad Sci U S A. 2002;99(23):14946–14951.

[45] Nakano Y, Jahan I, Bonde G, et al. A mutation in the Srrm4 gene causes alternative splicing defects and deafness in the Bronx waltzer mouse. PLoS Genet. 2012;8(10):e1002966.

[46] Nakano Y, Kelly MC, Rehman AU, et al. Defects in the alternative splicing-dependent regulation of REST cause deafness. Cell. 2018;174(3):536–48 e21.